The Canadian Mineralogist
Vol. 41, pp. 1241-1253 (2003)

OPTICAL, COMPOSITIONAL, MORPHOLOGICAL, AND X-RAY DATA ON ELEVEN PARTICLES OF AMPHIBOLE FROM LIBBY, MONTANA, U.S.A.

BRYAN R. BANDLI[¶] AND MICKEY E. GUNTER[§]

Department of Geological Sciences, University of Idaho, Moscow, Idaho 83844-3022, U.S.A.

BRENDAN TWAMLEY

University Research Office, University of Idaho, Moscow, Idaho 83844-3010, U.S.A.

FRANKLIN F. FOIT JR.

Department of Geology, Washington State University, Pullman, Washington 99164-2812, U.S.A.

SCOTT B. CORNELIUS

GeoAnalytical Laboratory, Washington State University, Pullman, Washington 99164-2812, U.S.A.

ABSTRACT

Amphibole crystals from the former vermiculite mine near Libby, Montana, were examined using three different analytical methods: optical and morphological measurements were made using spindle-stage methods, unit-cell refinements were performed using single-crystal X-ray-diffraction techniques, and chemical analyses were performed using an electron microprobe. The eleven samples display a continuum of morphology and conformity to a single crystal, and range from stubby single-crystal cleavage fragments to elongate near-bundles of fibers. Variations in conformity to the properties of a single crystal are reflected in the character of the X-ray reflections on X-ray rotation photographs. Using current nomenclature recommendations, all of the samples examined consist of winchite. Covariance among several properties was observed. The α index of refraction and birefringence are dependent on Mg content. There is also a correlation between birefringence and particle morphology. Winchite particles with a high birefringence and high width/thickness aspect ratio tend to be single crystals, whereas samples with a low birefringence and low width/thickness ratio tend to be more polycrystalline.

Keywords: winchite, electron-microprobe analysis, optical properties, amphibole asbestos, crystal morphology, Libby, Montana.

SOMMAIRE

Nous avons examiné des cristaux d'amphibole provenant de la mine de vermiculite près de Libby, au Montana, maintenant fermée, au moyen de trois méthodes analytiques, soit les mesures optiques et morphologiques effectuées avec une platine à aiguille, un affinement des paramètres réticulaires sur monocristal étudié en diffraction X, et une analyse chimique avec une microsonde électronique. Les onze échantillons font preuve d'une continuité en termes de morphologie et de conformité aux propriétés d'un monocristal; ils vont de fragments de clivage monocristallins trappus à des essaims allongés de fibres. Les variations en degré de conformité aux propriétés d'un monocristal se voient dans le caractère des réflexions en diffraction X sur des clichés de rotation. En termes des recommandations courantes de nomenclature, tous les échantillons sont de la winchite. Nous notons une covariance parmi plusieurs propriétés. L'indice de réfraction α et la biréfringence dépendent de la teneur en Mg. Il y a aussi une corrélation entre biréfringence et morphologie des particules. Les particules de winchite ayant une biréfringence élevée et un rapport de largeur à épaisseur élevé ont tendance à être des monocristaux, tandis que les échantillons ayant une faible biréfringence et un faible rapport de largeur à épaisseur seraient plutôt polycristallins.

(Traduit par la Rédaction)

Mots-clés: winchite, analyses à la microsonde électronique, propriétés optiques, amphibole asbestiforme, morphologie des cristaux, Libby, Montana.

[¶] *Present address*: MVA, Inc., 5500 Oakbrook Parkway, Suite 200, Norcross, Georgia 30093, U.S.A.
[§] *E-mail address*: mgunter@uidaho.edu

Introduction

In November of 1999, several articles in the popular press led the United States Environmental Protection Agency (EPA) to begin an investigation of asbestos-related diseases and remediation of asbestos contamination associated with the vermiculite mining and milling operations in Libby, Montana. Vermiculite was mined in an open-pit mine 9.6 km northeast of Libby from the early 1920s until the mine closed in 1990. Exfoliated vermiculite from Libby, known commercially as Zonolite, was produced by heating the ore. One of the major uses of this product was in attic insulation. At peak production, the mine accounted for approximately 80% of the world's production. Unfortunately, the vermiculite ore contained trace amounts of amphibole-asbestos (USEPA 2000). The amphibole-asbestos has been shown to cause asbestos-related lung disease in former mine and mill workers (Amandus & Wheeler 1987, Amandus *et al.* 1987a, b, McDonald *et al.* 1986a, b, 1988), and the health of the residents of Libby is currently being studied (USEPA 2001, ATSDR 2000, 2001).

Here, we present compositional and optical properties of amphiboles collected at the former mine site and discuss their relationship to variations in crystal morphology. Authors of two recent studies, Gunter *et al.* (2003) and Meeker *et al.* (2003), found the amphiboles at Libby to vary in morphology (*i.e.,* some individual samples contain both asbestiform and non-asbestiform amphiboles). In an earlier study, Gunter *et al.* (2001) found the amphiboles to be an approximately 50:50 mixture of asbestiform and non-asbestiform varieties. Authors of all three of these studies found that the majority of the amphibole present at the mine site is winchite; this species of amphibole-asbestos is not currently regulated by U.S. government agencies (OSHA 1986, 1992). They also found no correlation between composition and morphology. Our goal in this study is to provide optical, compositional, morphological, and structural data from a suite of samples collected at the former mine-site to better characterize the physical properties of these amphiboles, and to show gradational changes in these, as the samples become more polycrystalline.

Geological Context

The former mine is located in the Rainy Creek Complex, which is an ultramafic–alkaline intrusive complex composed of an altered biotite pyroxenite stock intruded by an irregular body of syenite. The ultramafic unit that makes up the stock was emplaced in the Precambrian Belt Supergroup during the Cretaceous period, followed by intrusion of the syenitic magma, which produced significant hydrothermal alteration of the ultramafic units (Boettcher 1967). Hydrothermal alteration of the biotite and its subsequent weathering to vermiculite resulted in one of the world's largest vermiculite deposits. Amphibole and amphibole-asbestos occur in the vermiculite ore as a product of the hydrothermal alteration of the pyroxene-group minerals (Boettcher 1966). For a more detailed discussion of the geology and mineralogy of the complex, see Bandli (2002).

Sample Selection

A suite of samples, collected by Gunter in October 1999 was taken from the center of the previous mining operation, in the biotite pyroxenite. Three samples of amphibole and amphibole-asbestos representing distinct geological occurrences (Fig. 1) were selected from this suite for further study. The first of these (termed "vein," Fig. 1A) is from a cross-fiber vein of amphibole approximately 2 cm wide cutting the biotite pyroxenite. The second (termed "outcrop," Fig. 1B) contains an intergrowth of pyroxenes that are altering to amphiboles. It was collected in place on a former mine bench. The last sample (termed "float," Fig. 1C), with a more massive morphology, is part of a 2–3 kg boulder. (These are the same suite of samples used in Gunter *et al.* 2003.) Three to four individual crystals were selected from each sample and are labeled alphabetically.

Experimental Methods

Eleven crystals of amphiboles were selected on the basis of their optical properties and morphological characteristics. Each was mounted on a glass fiber *ca.* 100 μm in diameter, fastened to an X-ray goniometer head for optical and X-ray studies. Variability in the morphology can be seen in Figure 2. Optical homogeneity was a prerequisite, and each of the eleven samples selected appeared as a single crystal when observed with the spindle stage – polarized light microscope combination (*i.e.,* the crystals exhibit sharp extinction positions and show no evidence of twinning). Index of refraction data were collected along with morphological measurements, both with the aid of a spindle stage. Next, the sample, mounted on an X-ray goniometer head, was transferred to a single-crystal X-ray diffractometer to obtain its unit-cell parameters. Finally, the single crystal was removed from the X-ray goniometer head, mounted in epoxy, and analyzed using an electron microprobe.

Optical measurements

Individual crystals were placed on a spindle stage attached to a Leitz Ortholux polarized light microscope. The orientations of the optical indicatrix and $2V$ were determined using the methods described in Bloss (1981) and the computer program EXCALIBR (Gunter & Twamley 2001) from data on extinction angles collected at spindle stage increments of 10° over the range 0–360°. Using these data, one can calculate with EXCALIBR the spindle stage and microscope stage

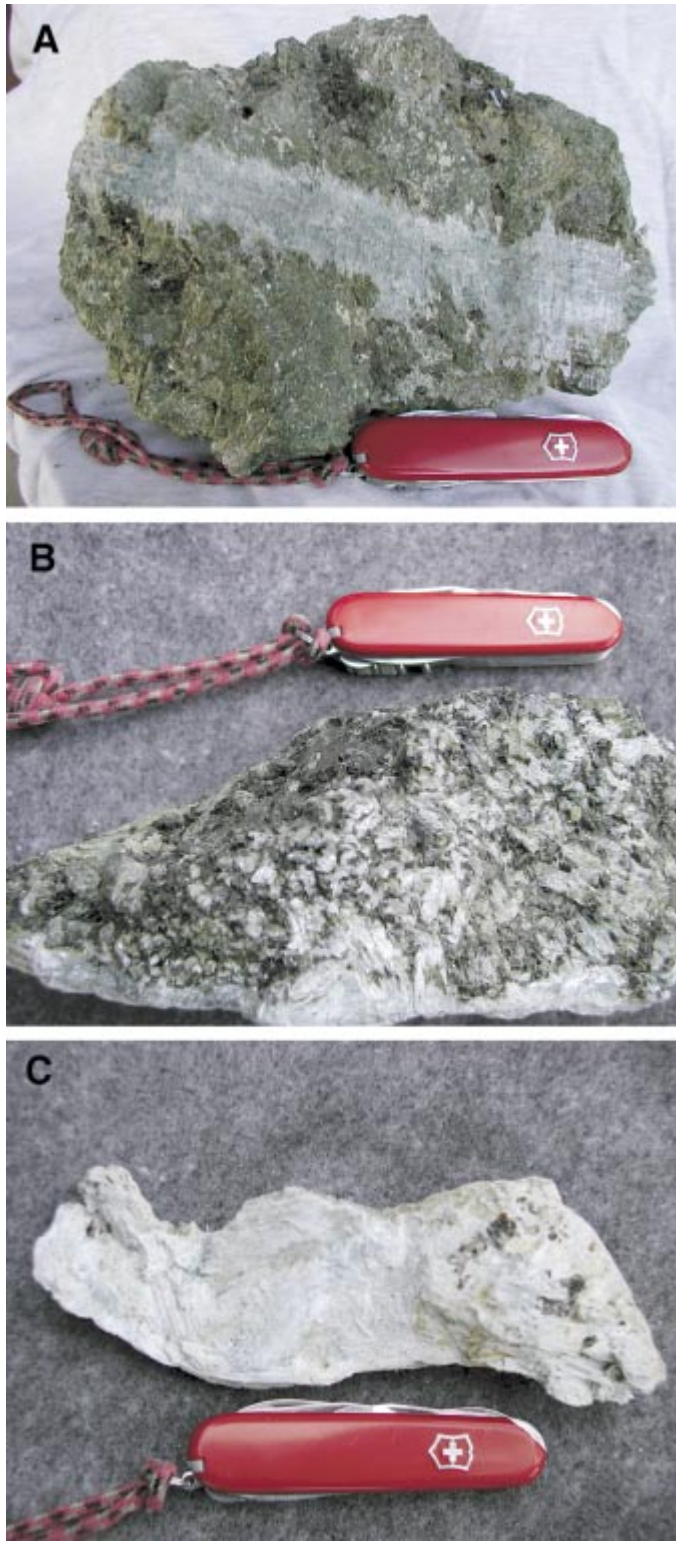

FIG. 1. Photographs of the three samples used in this study, collected at the former vermiculite mine near Libby. A. Vein of amphibole running through the host biotite pyroxenite. Single crystals were obtained from this vein and thus labeled "vein" in this study. B. Light-colored amphibole samples in a non-vein occurrence. This sample was collected in place, at a mine bench and thus termed "outcrop" in this study. The orientation of the amphibole crystals appears to be more random than in the "vein" sample in A. C. A portion of a fairly large boulder of amphibole collected from a float sample near the center of the mine, and in turn labeled "float." Pocket knife for scale in all photographs.

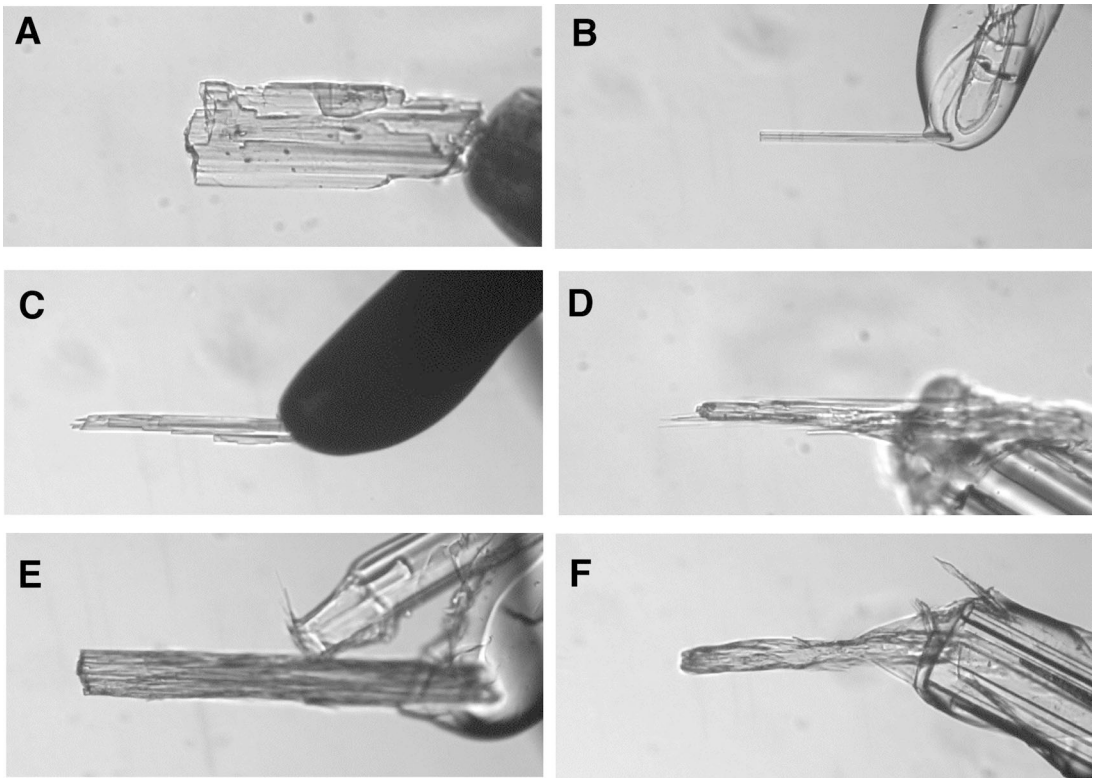

FIG. 2. Photomicrographs of amphibole fragments used in this study. The samples have been attached to approximately 100 μm glass fibers, and are in a 1.550 index of refraction liquid. Exact dimensions of the crystals are given in Table 1. These six samples are representative of the different morphologies in our suite, as discussed in the text. A. Sample "vein D" appears as a cleavage fragment of an amphibole; samples "outcrop C" and "float C" have a similar morphology. B. Sample "outcrop B" is a single crystal flattened on (100); samples "outcrop A" and "float B" have a similar morphology. C. Sample "float D" appears to be less monocrystalline than 2B; sample "vein B" has a similar morphology. D. Sample "vein C" appears less monocrystalline than 2C. E. Sample "vein A", is polycrystalline and was confirmed so by X-ray techniques. F. Sample "float A" is the most polycrystalline sample of the suite. See Table 1 for particle sizes.

settings needed to orient any direction of principal vibration (*i.e.,* α, β, γ) parallel to the microscope stage and parallel to the lower polarizer. This facilitates the measurement of indices of refraction without appreciable error due to misorientation. Indices of refraction were determined using the double variation method (Bloss 1981) and the computer program SOLID (Su *et al.* 1987). To increase the accuracy of these measurements, the Cargille index of refraction liquids were calibrated with an Abbe refractometer and the program OIL (Su *et al.* 1987), and then checked against standard glasses of known index of refraction. The precision and accuracy of measured indices of refraction is ±0.0005 (Bandli & Gunter 2001).

The dimensions of the crystals were measured to within ±1 μm using a Vickers image-splitting eyepiece. The spindle stage allows these measurements to be easily made because the sample can be rotated about the spindle axis. The crystals were first oriented with their longest dimension (*i.e.,* the *c* crystallographic axis) parallel to the rotation axis of the spindle stage. Next, the most narrow dimension (*i.e.,* the thickness) and longest dimension (*i.e.,* the width) were measured by rotation about the spindle axis.

X-ray measurements

Orientation matrices and unit-cell parameters were obtained at room temperature using a Bruker/Siemens SMART 1K single-crystal diffractometer and Mo$K\alpha$ radiation. Data were collected from 30–90 frames, with exposure times of 10–60 seconds per frame. The number of frames and the collection time for each frame were dependent on the size of each crystal. With the

orientation matrices from the X-ray diffractometer and from the spindle stage, the optical orientation of the mineral (*i.e., c*:Z) could be easily determined (Gunter & Twamley 2001).

Chemical analysis

Each of the single crystals was mounted in epoxy on a separate glass slide and ground on a lap wheel charged with 1200 grit to expose the crystal. The crystal was then polished successively with 3 μm and 1 μm diamond grit on a paper lap. The samples were analyzed at Washington State University in the Department of Geology's GeoAnalytical Laboratory using a Cameca Camebax electron microprobe employing wavelength-dispersion spectrometry (four spectrometers), an accelerating voltage of 15 kV, a beam current of 12 nA, and a beam diameter of 2 μm. Absorption, fluorescence, and atomic number corrections were applied to all data. The following elements (associated standards) were sought: Si and Al (Wilberforce hornblende), Ti (titanite), Fe (Rockport fayalite), Mn (spessartine), Mg (forsterite), Ca (diopside), K (orthoclase), Na (albite), Cl (KCl), and F (phlogopite). Fe was measured as FeO and apportioned to Fe^{2+} and Fe^{3+} using the ratio $Fe^{3+}/\Sigma Fe$ determined from Mössbauer spectroscopy (Gunter *et al.* 2003).

Results and Discussion

Chemical composition

Results of the electron-microprobe analyses are given in Table 1, as well as the $Fe^{3+}/\Sigma Fe$ values for the three types of sample (vein, outcrop, and float). Chlorine is not present in measurable amounts in any of the samples. Cation contents were calculated based on 24 (O, OH, F), the $Fe^{3+}/\Sigma Fe$ ratios from Mössbauer spectroscopy, and the assumption that OH + F = 2, (*i.e.,* the OH and, in turn, H_2O content were calculated by difference). Cation site assignments were made according to Leake *et al.* (1997) based on the general formula $A_{0-1}B_2C_5T_8O_{22}(OH,F)_2$. Following the recommendations of Leake *et al.* (1997), all eleven samples consist of a sodic–calcic amphibole (winchite) where $(Ca + Na)_B \geq 1$, $0.5 < Na_B < 1.5$, and *A*-site occupancy is less than 0.5. Elemental variation for the eleven samples in the non-tetrahedral cation contents is shown in Figure 3.

One of the issues surrounding the amphibole or amphibole-asbestos found at the former vermiculite mine at Libby, Montana is its mineralogical identity. Most investigators (including the popular press and U.S. regulatory agencies) have incorrectly referred to it as being either tremolite or actinolite (USEPA 2000). Wylie & Verkouteren (2000) cast doubt on this opinion when they identified two samples from the mine site as winchite, later confirmed by Gunter *et al.* (2003), who

TABLE 1A. CHEMICAL COMPOSITION, CHEMICAL FORMULAS*, SITE ASSIGNMENTS, INDICES OF REFRACTION, 2V, EXTINCTION ANGLES, CELL PARAMETERS, DIMENSION MEASUREMENTS, AND ASPECT RATIOS OF AMPHIBOLE PARTICLES TAKEN FROM VEIN SAMPLES

	vein A	vein B	vein C	vein D
SiO_2 wt.%	56.65(67)	56.92(46)	57.15(69)	56.12(55)
Al_2O_3	0.21(4)	0.14(3)	0.14(8)	0.34(9)
TiO_2	0.20(8)	0.21(8)	0.12(7)	0.21(9)
FeO	2.47(9)	2.38(16)	2.07(38)	2.08(18)
Fe_2O_3	4.98(19)	4.81(32)	4.19(76)	4.31(29)
MgO	20.05(15)	19.93(30)	20.36(1.38)	20.46(33)
MnO	0.11(2)	0.12(5)	0.12(2)	0.10(2)
CaO	6.44(73)	5.62(53)	9.23(61)	6.65(19)
Na_2O	4.24(31)	4.97(35)	3.28(40)	4.38(28)
K_2O	1.08(17)	1.43(13)	0.68(16)	1.22(12)
H_2O	1.91(3)	1.92(7)	2.02(5)	1.89(6)
F	0.47(5)	0.44(15)	0.28(12)	0.47(11)
Total	98.61(95)	98.72(50)	99.54(67)	98.04(50)
$Fe^{3+}/\Sigma Fe$	0.645	0.645	0.645	0.645
FeO_{EMPA}	6.95(26)	6.70(44)	5.84(1.06)	5.96(39)
# of analyses	8	10	9	8
Si *apfu*	7.98(2)	8.01(2)	7.96(4)	7.94(3)
Al	0.04(1)	0.02(0)	0.02(1)	0.06(2)
Ti	0.02(1)	0.02(1)	0.01(1)	0.02(1)
Fe^{2+}	0.29(1)	0.28(2)	0.24(5)	0.25(2)
Fe^{3+}	0.53(2)	0.51(4)	0.44(8)	0.46(3)
Mg	4.21(4)	4.18(5)	4.22(27)	4.32(5)
Mn	0.01(0)	0.01(1)	0.01(0)	0.01(0)
Ca	0.97(10)	0.85(8)	1.38(9)	1.01(3)
Na	1.16(9)	1.36(10)	0.89(11)	1.20(7)
K	0.19(3)	0.26(2)	0.12(3)	0.22(2)
H	1.79(2)	1.80(7)	1.87(5)	1.79(5)
F	0.21(2)	0.19(7)	0.13(5)	0.21(5)
T-Si	7.98	8.01	7.96	7.94
T-Al	0.02	-	0.02	0.06
T-Ti	-	-	0.01	-
Sum T	8.00	8.01	7.99	8.00
C-Al	0.02	0.02	-	-
C-Ti	0.02	0.02	-	0.02
C-Fe^{2+}	0.22	0.27	0.24	0.20
C-Fe^{3+}	0.53	0.51	0.44	0.46
C-Mg	4.21	4.18	4.22	4.32
C-Mn	-	-	0.01	-
Sum C	5	5.00	4.91	5.00
B-Fe^{2+}	0.07	0.01	-	0.05
B-Mn	0.01	0.01	-	0.01
B-Ca	0.97	0.85	1.38	1.01
B-Na	0.95	1.13	0.62	0.93
Sum B	2.00	2.00	2.00	2.00
A-Na	0.21	0.23	0.27	0.27
A-K	0.19	0.26	0.12	0.22
Sum A	0.40	0.49	0.39	0.49
α	1.6265(5)	1.6251(4)	1.6221(14)	1.6214(4)
β	1.6349(6)	1.6345(5)	1.6316(6)	1.6340(5)
γ	1.6381(10)	1.6389(8)	1.6387(5)	1.6397(5)
$2V_x$ ° obs.	58(1)	64(2)	73(2)	63(1)
a (Å)	-	-	-	9.891(4)
b (Å)	-	-	-	17.969(9)
c (Å)	-	-	-	5.266(2)
β °	-	-	-	104.73(3)
c:Z_{calc} °	-	-	-	21
length (μm)	605	486	319	278
width (μm)	88	58	22	95
thickness (μm)	52	30	18	35
l/w	6.9	8.4	14.5	2.9
l/t	11.6	16.2	17.7	7.9
w/t	1.7	1.9	1.2	2.7

* Based on 24 O, OH, F per formula unit.

TABLE 1B. CHEMICAL COMPOSITION, CHEMICAL FORMULAS*, SITE ASSIGNMENTS, INDICES OF REFRACTION, 2V, EXTINCTION ANGLES, CELL PARAMETERS, DIMENSION MEASUREMENTS, AND ASPECT RATIOS OF AMPHIBOLE PARTICLES TAKEN FROM OUTCROP SAMPLES

	outcrop A	outcrop B	outcrop C
SiO_2 wt.%	56.64(75)	57.01(82)	56.39(52)
Al_2O_3	0.13(2)	0.18(3)	0.20(7)
TiO_2	0.04(2)	0.04(2)	0.04(3)
FeO	1.82(15)	1.84(9)	2.16(32)
Fe_2O_3	4.57(36)	4.62(21)	5.43(81)
MgO	20.48(20)	20.38(32)	20.06(66)
MnO	0.24(5)	0.20(2)	0.12(3)
CaO	9.24(51)	7.81(24)	7.32(92)
Na_2O	2.85(16)	3.71(19)	4.03(40)
K_2O	0.74(4)	0.94(6)	0.86(11)
H_2O	1.92(5)	1.88(5)	1.90(8)
F	0.46(10)	0.55(9)	0.49(13)
Total	98.95(80)	98.94(95)	98.80(83)
$Fe^{3+}/\Sigma Fe$	0.693	0.693	0.693
FeO_{EMPA}	5.94(47)	5.99(28)	7.05(1.05)
# of analyses	8	7	9
Si *apfu*	7.94(4)	7.98(5)	7.94(2)
Al	0.02(0)	0.03(0)	0.03(1)
Ti	0.00(0)	0.00(0)	0.00(0)
Fe^{2+}	0.21(2)	0.22(1)	0.25(4)
Fe^{3+}	0.48(4)	0.49(3)	0.58(9)
Mg	4.28(7)	4.25(5)	4.21(10)
Mn	0.03(1)	0.02(1)	0.01(0)
Ca	1.39(8)	1.17(3)	1.10(13)
Na	0.77(4)	1.01(6)	1.10(11)
K	0.13(1)	0.17(1)	0.16(2)
H	1.79(5)	1.75(4)	1.78(6)
F	0.20(5)	0.25(4)	0.22(6)
T-Si	7.94	7.98	7.94
T-Al	0.02	0.02	0.03
T-Ti	-	-	-
Sum T	7.96	8.00	7.97
C-Al	-	0.01	-
C-Ti	-	-	-
C-Fe^{2+}	0.21	0.22	0.21
C-Fe^{3+}	0.48	0.49	0.58
C-Mg	4.28	4.25	4.21
C-Mn	0.03	0.02	-
Sum C	5.00	4.99	5.00
B-Fe^{2+}	-	-	0.04
B-Mn	-	-	0.01
B-Ca	1.39	1.17	1.10
B-Na	0.61	0.83	0.85
Sum B	2.00	2.00	2.00
A-Na	0.16	0.18	0.25
A-K	0.13	0.17	0.16
Sum A	0.29	0.35	0.41
α	1.6238(4)	1.6228(11)	1.6243(9)
β	1.6329(4)	1.6305(5)	1.6323(5)
γ	1.6392(7)	1.6388(12)	1.6417(4)
$2V_x$ ° obs.	63(1)	66(1)	67(1)
a (Å)	9.906(4)	9.769(4)	9.94(1)
b (Å)	18.010(8)	17.982(7)	18.27(2)
c (Å)	5.306(1)	5.265(2)	5.278(2)
β °	105.07(3)	104.39(1)	104.72(7)
$c:Z_{calc}$ °	22(obs)	21	-
length (μm)	230	372	222
width (μm)	25	24	110
thickness (μm)	7	11	33
l/w	9.2	15.5	2.0
l/t	32.9	33.8	6.7
w/t	3.6	2.2	3.3

* Based on 24 O, OH, F per formula unit.

TABLE 1C. CHEMICAL COMPOSITION, CHEMICAL FORMULAS*, SITE ASSIGNMENTS, INDICES OF REFRACTION, 2V, EXTINCTION ANGLES, CELL PARAMETERS, DIMENSION MEASUREMENTS, AND ASPECT RATIOS OF AMPHIBOLE PARTICLES TAKEN FROM FLOAT SAMPLES

	float A	float B	float C	float D
SiO_2 wt.%	57.14(49)	56.29(61)	56.29(61)	57.18(73)
Al_2O_3	0.20(4)	0.33(7)	0.14(6)	0.18(4)
TiO_2	0.25(4)	0.13(3)	0.08(3)	0.25(17)
FeO	2.11(19)	1.26(7)	1.77(23)	1.60(21)
Fe_2O_3	6.16(55)	3.68(20)	5.16(67)	4.67(62)
MgO	19.21(42)	21.36(20)	20.01(51)	20.47(43)
MnO	0.05(3)	0.12(3)	0.05(2)	0.09(1)
CaO	5.52(62)	8.63(21)	7.26(64)	7.63(30)
Na_2O	3.53(37)	3.40(17)	3.60(57)	3.76(20)
K_2O	0.72(5)	0.92(5)	0.72(8)	0.79(10)
H_2O	1.97(6)	1.91(5)	1.96(2)	1.98(4)
F	0.30(11)	0.47(10)	0.31(4)	0.34(11)
Total	97.05(79)	98.50(61)	97.24(97)	98.80(65)
$Fe^{3+}/\Sigma Fe$	0.724	0.724	0.724	0.724
FeO_{EMPA}	7.65(69)	4.62(25)	6.41(83)	5.80(77)
# of analyses	6	8	7	8
Si *apfu*	8.10(4)	7.91(3)	8.00(4)	7.99(4)
Al	0.03(1)	0.05(1)	0.02(1)	0.03(1)
Ti	0.03(0)	0.01(0)	0.01(0)	0.03(2)
Fe^{2+}	0.25(2)	0.15(1)	0.21(3)	0.19(3)
Fe^{3+}	0.66(5)	0.39(2)	0.55(7)	0.49(7)
Mg	4.06(10)	4.47(3)	4.24(11)	4.26(6)
Mn	0.01(0)	0.01(0)	0.01(0)	0.01(0)
Ca	0.84(10)	1.30(3)	1.11(10)	1.14(4)
Na	0.97(10)	0.93(5)	0.99(16)	1.02(6)
K	0.13(1)	0.17(1)	0.13(1)	0.14(2)
H	1.86(5)	1.79(5)	1.86(2)	1.85(5)
F	0.13(5)	0.21(5)	0.14(2)	0.15(5)
T-Si	8.10	7.91	8.00	7.99
T-Al	-	0.05	-	0.01
T-Ti	-	0.01	-	-
Sum T	8.10	7.97	8.00	8.00
C-Al	0.03	-	0.02	0.02
C-Ti	0.03	-	0.01	0.03
C-Fe^{2+}	0.22	0.14	0.18	0.19
C-Fe^{3+}	0.66	0.39	0.55	0.49
C-Mg	4.06	4.47	4.24	4.26
C-Mn	-	-	-	0.01
Sum C	5.00	5.00	5.00	5.00
B-Fe^{2+}	0.03	0.01	0.03	-
B-Mn	0.01	0.01	0.01	-
B-Ca	0.84	1.30	1.11	1.14
B-Na	0.97	0.68	0.85	0.86
Sum B	1.85	2.00	2.00	2.00
A-Na	-	0.25	0.14	0.16
A-K	0.13	0.17	0.13	0.14
Sum A	0.13	0.42	0.27	0.30
α	1.6253(49)	1.6177(6)	1.6226(10)	1.6257(5)
β	1.6305(3)	1.6351(5)	1.6342(7)	1.6370(6)
γ	1.6337(12)	1.6369(6)	1.6391(6)	1.6407(4)
$2V_x$ ° obs.	80(1)	67(1)	60(1)	59(1)
a (Å)	-	-	9.849(4)	9.862(3)
b (Å)	-	-	17.994(6)	18.075(4)
c (Å)	-	-	5.287(2)	5.290(1)
β °	-	-	104.38(3)	104.56(2)
$c:Z_{calc}$ °	-	-	22	-
length (μm)	528	227	151	392
width (μm)	50	13	46	46
thickness (μm)	47	6	19	20
l/w	10.6	17.5	3.3	8.5
l/t	11.2	37.8	8.0	19.6
w/t	1.0	2.2	2.4	2.3

* Based on 24 O, OH, F per formula unit.

also reported the "vein" sample to consist of richterite with an average *A*-site occupancy of 0.52 atoms. Also, Meeker *et al.* (2003) showed that the majority of thirty samples they collected consist of winchite. Both the "outcrop" and "float" samples were found to be winchite with average *A*-site occupancies of 0.35 and 0.34 atoms per formula unit (*apfu*), respectively. In this study, we found four crystals from the "vein" sample, three crystals from the "outcrop" sample, and four crystals from the "float" sample to be winchite, with average *A*-site occupancies of 0.44, 0.35, 0.28 *apfu*, respectively. Thus, the compositional data in this study agree, within experimental error, with those in Gunter *et al.* (2003).

The two elements that seem to vary the most in the winchite crystals studied here are Mg and Ca, and even for these the variability is small. The average proportion of Mg for the "vein" samples is 4.23 *apfu*; in the "outcrop" samples, it is 4.24 *apfu*, and in the "float" samples, it is 4.25 *apfu*; this compares to 4.21, 4.17, and 4.32 *apfu*, respectively, for the "vein", "outcrop", and "float" in Gunter *et al.* (2003). The Ca values are also similar, for instance, the Ca values for the three samples in this study are 1.05, 1.22, and 1.10 *apfu*, respectively, for the "vein", "float", and "outcrop" samples, compared to 0.91, 1.14, and 1.20 from Gunter *et al.* (2003).

Optics

Indices of refraction and $2V$ are also given in Table 1. All samples are optically negative, with $2V_x$ ranging from 58 to 80°. Indices of refraction vary over the range 1.6177–1.6265 for α, 1.6305–1.6370 for β, and 1.6337–1.6417 for γ (Fig. 4), and their variation with Mg content is shown in Figure 5. The sample "float A" is excluded from the linear regression equations for two reasons. First, if a regression line is fit to the central cluster of data, it does not extend to include the "float A" point. The line does include the point representing the sample "float B", however, and it is included in the regression equation. Secondly, the "float A" sample is optically and morphologically unique in this group of samples. It has the lowest value of birefringence by far of any of the samples, and it also appears to be the most polycrystalline. These two factors led us to exclude the "float A" sample from the regression analysis.

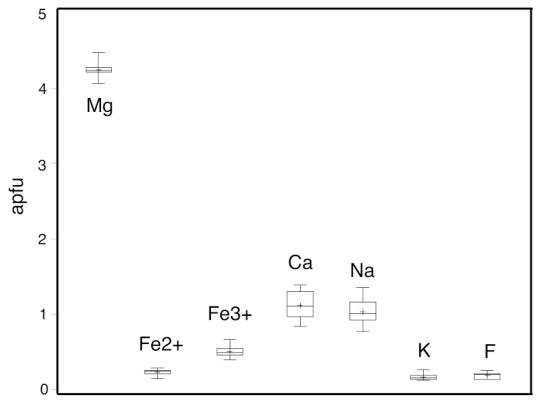

FIG. 3. Boxplots showing the variability in the calculated amounts of the ions Mg, Fe^{2+}, Fe^{3+}, Ca, Na, K, and F for the samples in this study expressed in atoms per formula unit (*apfu*). The raw data for this plot are given in Table 1. The boxplot shows the median of the data represented by a cross, the mean with a horizontal line, the upper and lower 25th percentile of the data is contained within the box, and the whiskers extend out to the maximum and minimum values.

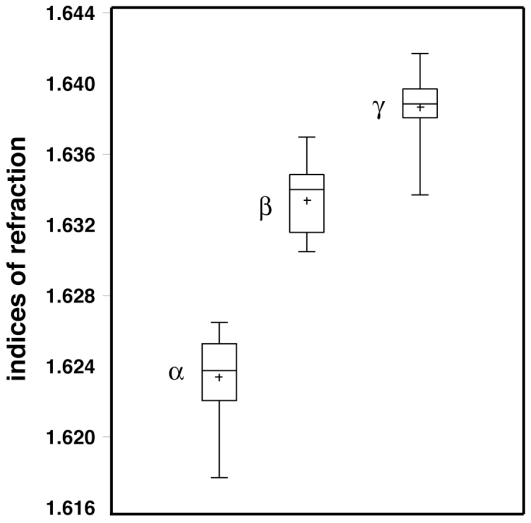

FIG. 4. Boxplots showing the variability in the measurements of the indices of refraction α, β, and γ for the samples in this study. The raw data for this plot are given in Table 1.

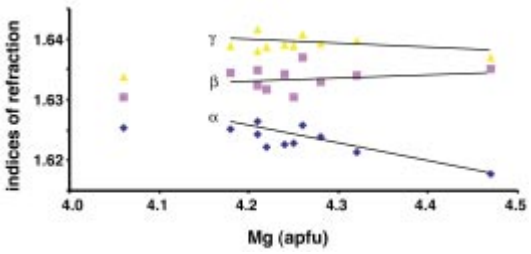

FIG. 5. Plot showing the dependence of indices of refraction on Mg content. Regression lines were calculated excluding sample float A (Mg = 4.06). The regression equations are given in Table 3.

As expected on the basis of such small chemical variations, there are only small variations in the indices of refraction, on the order of ±0.005. The only significant correlation between indices of refraction and composition involves Mg (Table 2) and Fe. Since Mg yielded better regression models than Fe, we chose to model the optical data based on Mg. Figure 5 is a plot of the three indices of refraction *versus* Mg content, and the linear regression equations are given in Table 3. Of these, α is the most sensitive to compositional variation. We excluded the "float A" sample from the regression because it appeared to be an outlier, and it is morphologically distinct from the other samples (Fig. 2F). Birefringence changes significantly as a function of Mg content (Figs. 5, 6), and this relationship is modeled with the regression equations in Table 3. Again, the "float A" sample is plotted but not included in the regression analysis. Figure 6 shows that both the total birefringence (*i.e.,* γ–α) and partial birefringence (*i.e.,* β–α) are positively correlated with Mg content.

TABLE 2. CORRELATION COEFFICIENTS FOR THE COVARIANCE BETWEEN INDICES OF REFRACTION AND Mg CONTENT OF ELEVEN PARTICLES OF AMPHIBOLE, LIBBY, MONTANA

	α	β	γ	Mg
γ – α	-0.85	-0.20	0.04	0.67
	(0.00)	(0.57)	(0.99)	(0.04)
β – α	-0.77	0.52	-0.45	0.88
	(0.00)	(0.13)	(0.19)	(0.00)
Mg	-0.88	0.25	-0.48	1
	(0.00)	(0.49)	(0.16)	

Values listed in parentheses under the correlation coefficients are a test statistic to determine if the correlation coefficient is significant (*i.e.,* the smaller the value of the test statistic, the more significant the value of the correlation coefficient). Note that sample "float A" is excluded from the analysis.

Morphology

Figure 2 is a series of photomicrographs showing six of the eleven samples examined and the trend in particle morphology from well-crystallized fragments to more poorly crystallized particles that appear somewhat polycrystalline (Figs. 2A–F). Figure 2A is a cleavage fragment from the "vein D" sample. Both the "outcrop C" and "float D" samples are morphologically similar to this fragment. Figure 2B shows an amphibole particle ("outcrop B") flattened on (100), which is typical for small particles of amphibole (Dorling & Zussman 1987). Samples "outcrop A" and "float B" share this morphology. Figure 2C shows a morphology departing slightly more from that of a single crystal than that in Figure 2B. However, we obtained unit-cell parameters for this sample ("float D"), verifying that it is a single crystal. Sample "vein B" shares this morphology. Figure 2D ("vein C") shows a morphology appearing to depart even more from that of a single crystal than in Figure 2C, which did not yield unit-cell parameters. This is the only sample displaying this morphology. The "vein A" sample (Fig. 2E) and the "float A" sample (Fig. 2F) have X-ray-diffraction patterns (see below)

TABLE 3. LINEAR REGRESSION EQUATIONS RELATING INDICES OF REFRACTION, (γ – α) AND (β – α) TO Mg CONTENT, AND MULTIPLE LINEAR REGRESSION EQUATIONS FOR (γ – α) AND (β – α) WITH Mg AND MORPHOLOGY OF ELEVEN PARTICLES OF AMPHIBOLE FROM LIBBY, MONTANA

$\alpha =$	$1.73(3) - 0.025(6)Mg$	$R^2 = 0.69$	$F = 17.89$	$Pr > F = 0.003$
	$<0.0001 \quad 0.0029$			
$\beta =$	$1.61(3) + 0.006(8)Mg$	$R^2 = 0.06$	$F = 0.5$	$Pr > F = 0.49$
	$<0.0001 \quad 0.4929$			
$\gamma =$	$1.67(2) - 0.008(5)Mg$	$R^2 = 0.24$	$F = 2.39$	$Pr > F = 0.16$
	$<0.0001 \quad 0.1604$			
$\gamma - \alpha =$	$-0.06(3) + 0.018(8)Mg$	$R^2 = 0.44$	$F = 6.38$	$Pr > F = 0.0355$
	$0.0815 \quad 0.0355$			
$\gamma - \alpha =$	$0.022(9)Mg - 0.00005(1)l/t - 0.08(4)$	$R^2 = 0.50$	$F = 3.51$	$Pr > F = 0.0878$
	$0.0372 \quad 0.3995 \quad 0.0696$			
$\beta - \alpha =$	$-0.12(3) + 0.031(6)Mg$	$R^2 = 0.78$	$F = 21.78$	$Pr > F = 0.008$
	$0.0013 \quad 0.0008$			
$\beta - \alpha =$	$0.038(6)Mg - 0.00008(4)l/t - 0.15(3)$	$R^2 = 0.85$	$F = 19.47$	$Pr > F = 0.0014$
	$0.0006 \quad 0.1138 \quad 0.0008$			

Values appearing under the terms in the regression equations are test statistics as defined in Table 2. Note that sample "float A" was excluded from the analysis.

characteristic of polycrystalline samples and thus did not yield unit-cell parameters. There is clearly a gradational change in morphology from Figure 2A to Figure 2F. Notably, Figure 2A, 2D, and 2E show crystals from the "vein" sample in Figure 1A; thus, crystals from the same specimen can have strikingly different morphologies.

The dimensions of the individual crystals and their aspect ratios (l/w, l/t, and w/t) are given in Table 1. Variability in the length, width, and thickness for the eleven samples is shown in Figure 7, and the variability in the aspect ratios is recorded in Figures 8 and 9. Figure 9, which is arranged with the width/thickness ratio increasing to the right, shows significant variation in the aspect ratios for the eleven samples. Also shown in Figure 9 are photos of all eleven particles. It is clear from these photos that the morphology changes as a function of the w/t aspect ratio. In our study, higher width/thickness ratios correspond to crystal fragments, whereas lower width/thickness ratios correspond to samples that are more polycrystalline. The correlation-coefficient matrix (Table 4) relating the morphological measurements shows a high positive correlation between the width and the thickness, and high negative

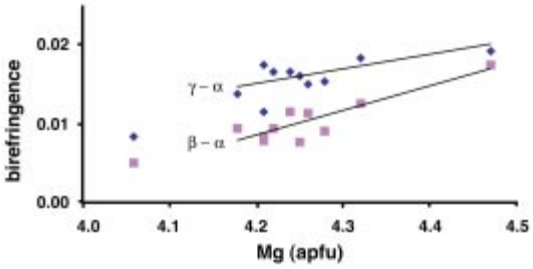

FIG. 6. Plot showing dependence of birefringence and partial birefringence on Mg content for the samples in this study. Regression lines were calculated excluding sample float A (Mg = 4.06). The egression equations are given in Table 3.

TABLE 4. CORRELATION COEFFICIENTS FOR PARTICLE DIMENSIONS AND ASPECT RATIOS OF THE ELEVEN PARTICLES USED IN THIS STUDY

	l	w	t	l/w	l/t	w/t
l	1					
w	0.18	1				
	(0.60)					
t	0.68	0.75	1			
	(0.02)	(0.01)				
l/w	0.13	-0.83	-0.50	1		
	(0.69)	(0.00)	(0.12)			
l/t	-0.16	-0.78	-0.76	0.80	1	
	(0.63)	(0.00)	(0.01)	(0.00)		
w/t	-0.64	0.25	-0.37	-0.45	0.12	1
	(0.03)	(0.46)	(0.26)	(0.16)	(0.72)	

Values appearing under the terms in the regression equations are test statistics as defined in Table 2. Note that sample "float A" was excluded from the analysis.

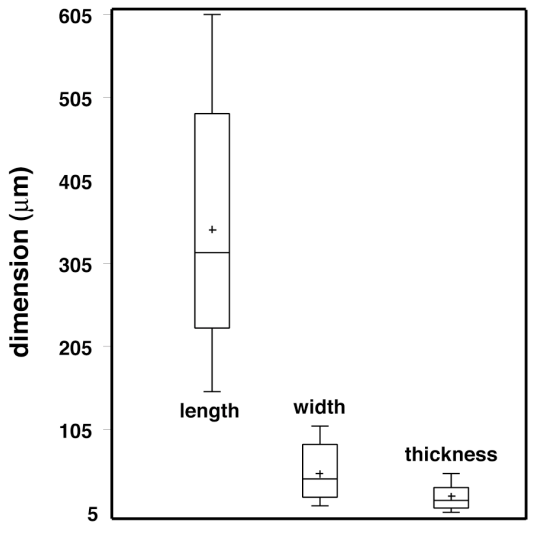

FIG. 7. Boxplots showing the variability in the measurements of the dimensions length, width, and thickness for the samples in this study.

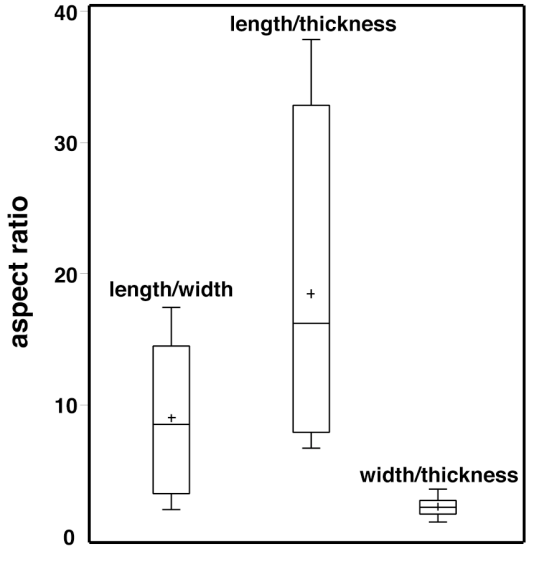

FIG. 8. Boxplots showing the variability in the aspect ratios length/width, length/thickness, and width/thickness for the samples in this study.

correlations between the width and length/width, the width and length/thickness, and the thickness and length/thickness. Interestingly, length shows no correlation to width or to the length/width ratio, which is contrary to what is normally observed in aspect-ratio correlations in asbestos minerals (Wylie 1988, 1993, Wylie & Schweitzer 1982).

X-ray diffraction

Unit-cell parameters (Table 1) for six of the eleven samples were refined from single-crystal diffraction data. Five crystals did not yield adequate X-ray-diffraction data to obtain unit-cell parameters. The "float B" sample consists of a small crystal of amphibole in the fingernail polish used to affix the sample to the glass fiber. Although this did not interfere with collection of optical data, it interfered with collection of X-ray-diffraction data. Also, the "vein B" sample was slightly bent, and the "float A", "vein C", and "vein A" are polycrystalline aggregates, which resulted in insufficient data for refinement of unit-cell parameters. All crystals display *C*2/*m* space-group symmetry, with unit-cell parameters varying over the following ranges: $9.77 < a < 9.93$, $17.96 < b < 18.27$, $5.27 < c < 5.31$ Å, and $104.38 < \beta < 105.07°$. No covariance between unit-cell parameters and any other measured property, including compositional parameters, was observed.

Integration of optical and X-ray data allows for determination of *c*:Z using the methods described in Gunter & Twamley (2001). For the six samples whose orientation matrices were determined, their *c*:Z values ranged between 21 and 22° (Table 1). Note that out of six samples, two yielded inconsistent results, possibly

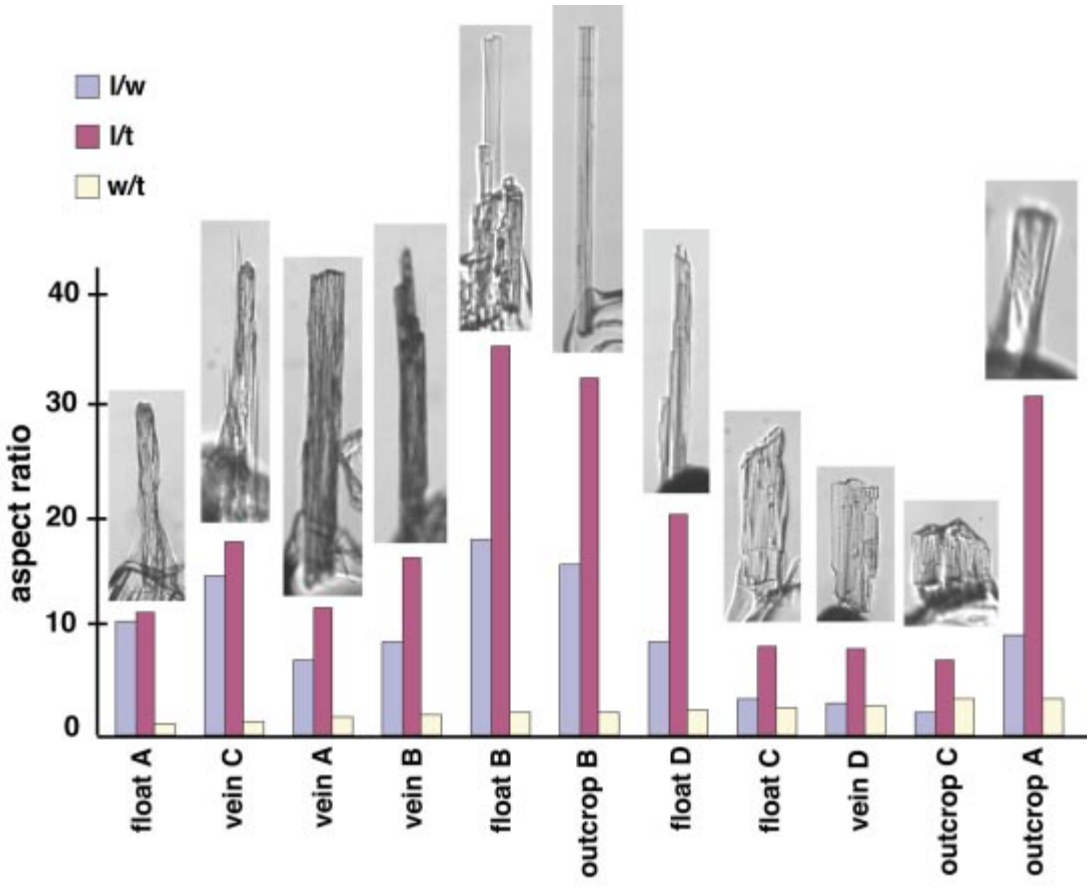

FIG. 9. Bar graph showing aspect ratios length/width (l/w), length/thickness (l/t), and width/thickness (w/t). Samples are arranged with the lowest w/t aspect ratio samples on the left and the highest w/t ratio samples on the right. Also a small photomicrograph of each of the eleven particles is shown. See Table 1 for particle sizes.

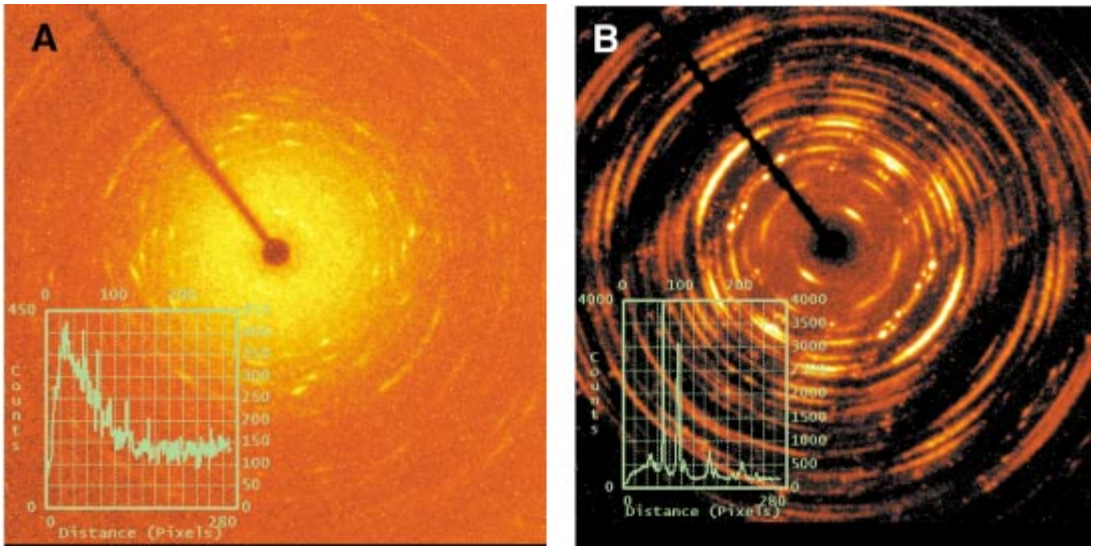

FIG. 10. X-ray rotation photographs of crystalline and fibrous samples. A. X-ray rotation photograph of a crystalline sample, similar in morphology to Figure 2C. Note presence of diffraction spots. B. X-ray rotation photograph of a more polycrystalline sample, similar in morphology to Figure 2E. Note the smearing of diffraction spots into semicircles. Inset images in the lower left of A and B represent a diffraction intensity cross-section from the photo's center to its edge. In A, only scattered radiation occurs (*i.e.*, the cross-section does not pass through any diffraction spots), whereas in B, the smeared-out diffraction spots simulate a powder-diffraction pattern obtained from the single polycrystalline particle.

because the samples moved on the glass fibers between the sets of measurements.

Rotation photographs of two samples were obtained using a SMART 1K CCD X-ray camera. Figure 10A is a rotation photograph of a sample similar in morphology to that shown in Figure 2C, and it shows individual reflections characteristic of single crystals. Figure 10B is an X-ray rotation photograph of a sample similar in morphology to Figure 2E. In this photograph, the reflections are smeared into arcs, which is characteristic of polycrystalline materials. Thus, morphological characteristics observed using the light microscope are confirmed in X-ray-diffraction patterns. Despite the fact that several of our samples did not yield sufficiently high-quality diffraction data to obtain unit cell-parameters, they did provide good-quality extinction datasets that could be processed by EXCALIBR to arrive at an optical orientation matrix.

Correlation among chemical, optical, and morphological properties

Previous studies have shown that the amphibole asbestos minerals can appear optically uniaxial (Dorling & Zussman 1987) as α and β indices of refraction tend to become equal. This equality occurs because there is a radial distribution of the α and β indices of refraction with reference to the γ index of refraction (*i.e.,* the index of refraction near parallel to *c*). Thus, one would expect a continuum in birefringence, with birefringence decreasing as the polycrystalline character of the particle increases. However, as was previously shown, the birefringence also changes as a function of composition. Thus, both composition and morphology control the birefringence, and this relationship is defined by the multiple linear regressions in Table 3.

The relationship between polycrystallinity and the width/thickness (w/t) aspect ratio can be determined by comparing w/t ratios in Figure 9 to the photographs of the particles in Figure 2 and noting which of the single crystals yielded unit-cell parameters. Samples "float A", "vein C" and "vein A" (Fig. 9) did not yield unit-cell parameters and thus are more strongly polycrystalline than the other samples and have lower values of the width/thickness aspect ratio, indicating they are more strongly fibrous in nature. This change in morphology can also be observed in the photomicrographs of these particles in Figure 2, where Figure 2D is sample "vein C", Figure 2E is sample "vein A", and Figure 2F is sample "float A". The remaining samples, all with higher width/thickness values, also yielded unit-cell parameters, confirming that they are single crystals.

Summary

Electron-microprobe analysis of amphibole fragments from the former vermiculite mine at Libby, Montana showed the amphibole should be classified as winchite (Leake *et al.* 1997). Optical, chemical, and X-ray-diffraction studies of these winchite samples reveal a covariance between optical properties and composition and morphological characteristics. The α index of refraction and birefringence are both dependent on Mg content. Birefringence is also dependent on the width/thickness aspect ratio of a sample. Winchite samples with a high birefringence and a high width/thickness aspect ratio tend to be well crystallized, whereas samples with low birefringence and a low width/thickness aspect ratio are more strongly polycrystalline. In this group of samples, there is no correlation between length/width aspect ratio and the degree of conformity to the properties of a single crystal.

Acknowledgements

The authors acknowledge the helpful reviews received from Antonio Gianfagna and an anonymous referee. David Berkoff assisted in the collection of samples.

References

Agency for Toxic Substances and Disease Registry (2000): Health consultation, Libby asbestos site, Libby, Lincoln County, Montana. Mortality from asbestosis in Libby, Montana, 1979–1998, December 12, 2000. Agency for Toxic Substances and Disease Registry, Atlanta, Georgia.

Agency for Toxic Substances and Disease Registry (2001): Year 2000 medical testing of individuals potentially exposed to asbestiform minerals associated with vermiculite in Libby, Montana, a report to the community. Agency for Toxic Substances and Disease Registry, Division of Health Studies, U.S. Department of Health and Human Services, Atlanta, Georgia.

Amandus, H.E., Althouse, R., Morgan, W.K.C., Sargent, E.N. & Jones, R. (1987b): The morbidity and mortality of vermiculite miners and millers exposed to tremolite-actinolite. III. Radiographic findings. *Am. J. Indust. Med.* **11**, 27-37.

_____ & Wheeler, R. (1987): The morbidity and mortality of vermiculite miners and millers exposed to tremolite-actinolite. II. Mortality. *Am. J. Indust. Med.* **11**, 15-26.

_____, _____, Jankovic, J. & Tucker, J. (1987a): The morbidity and mortality of vermiculite miners and millers exposed to tremolite–actinolite. I. Exposure estimates. *Am. J. Indust. Med.* **11**, 1-14.

Bandli, B.R. (2002): *Characterization of Amphibole and Amphibole-Asbestos from the Former Vermiculite Mine at Libby, Montana*. M.S. thesis, University of Idaho, Moscow, Idaho.

_____ & Gunter, M.E. (2001): Identification and characterization of mineral and asbestos particles using the spindle stage and the scanning electron microscope: the Libby, Montana, U.S.A. amphibole-asbestos as an example. *Microscope* **49**, 191-199.

Bloss, F.D. (1981): *The Spindle Stage: Principles and Practice*. Cambridge University Press, Cambridge, U.K.

Boettcher, A.L. (1966): Vermiculite, hydrobiotite, and biotite in the Rainy Creek igneous complex near Libby, Montana. *Clay Minerals* **6**, 283-296.

_____ (1967): The Rainy Creek alkaline-utramafic igneous complex near Libby, Montana. I. Ultramafic rocks and fenite. *J. Geol.* **75**, 526-553.

Dorling, M. & Zussman, J. (1987): Characteristics of asbestiform and non-asbestiform calcic amphiboles. *Lithos* **20**, 469-489.

Gunter, M.E., Brown, B.M., Bandli, B.R. & Dyar, M.D. (2001): Amphibole-asbestos, vermiculite mining, and Libby, Montana: what's in a name? Eleventh Goldschmidt Conference, Hot Springs, Virginia.

_____, Dyar, M.D., Twamley, B., Foit, F.F., Jr. & Cornelius, S. (2003): Composition, $Fe^{3+}/\Sigma Fe$, and crystal structure of non-asbestiform and asbestiform amphiboles from Libby, Montana, U.S.A. *Am. Mineral.* **88**, 1970-1978.

_____ & Twamley, B. (2001): A new method to determine the optical orientation of biaxial minerals: a mathematical approach. *Can. Mineral.* **39**, 1701-1711.

Leake, B.E., Woolley, A.R., Arps, C.E.S., Birch, W.D., Gilbert, M.C., Grice, J.D., Hawthorne, F.C., Kato, A., Kisch, H.J., Krivovichev, V.G., Linthout, K., Laird, J., Mandarino, J.A., Maresch, W.V., Nickel, E.H., Rock, N.M.S., Schumacher, J.C., Smith, D.C., Stephenson, N.C.N., Ungaretti, L., Whittaker, E.J.W. & Youzhi, G. (1997): Nomenclature of the amphiboles: report of the subcommittee on amphiboles of the International Mineralogical Association, Commission on New Minerals and Mineral Names. *Can. Mineral.* **35**, 219-246.

McDonald, J.C., McDonald, A.D., Armstrong, B. & Sébastien, P. (1986a): Cohort study of the mortality of vermiculite miners exposed to tremolite. *Brit. J. Indust. Med.* **43**, 436-444.

_____, _____, Sébastien, P. & Moy, K. (1988): Health of vermiculite miners exposed to trace amounts of fibrous tremolite. *Brit. J. Indust. Med.* **45**, 630-634.

_____, Sébastien, P. & Armstrong, B. (1986b): Radiological survey of past and present vermiculite miners exposed to tremolite. *Brit. J. Indust. Med.* **43**, 445-449.

MEEKER, G.P., BERN, A.M., BROWNFIELD, I.K., LOWERS, H.A., SUTLEY, S.J., HOEFEN, T.M. & VANCE, J.S. (2003): The composition and morphology of amphibole from the Rainy Creek Complex, near Libby, Montana. *Am. Mineral.* **88**, 1955-1969.

OCCUPATIONAL SAFETY AND HEALTH ADMINISTRATION (1986): Occupation exposure to asbestos, tremolite, anthophyllite, and actinolite. 29 CFR 1910.1001 and 29 CFR 1926.58. United States Government.

OCCUPATIONAL SAFETY AND HEALTH ADMINISTRATION (1992): OSHA Preambles: Asbestos [1992-Original standard]. United States Government.

SU, SHU-CHUN, BLOSS, F.D. & GUNTER, M. (1987): Procedures and computer programs to refine the double-variation method. *Am. Mineral.* **72**, 1011-1013.

UNITED STATES ENVIRONMENTAL PROTECTION AGENCY (2000): *Sampling and analysis of consumer garden products that contain vermiculite*. Report 2001-S-7. United States Environmental Protection Agency, Washington D.C.

UNITED STATES ENVIRONMENTAL PROTECTION AGENCY (2001): *EPA's actions concerning asbestos-contaminated vermiculite in Libby, Montana*. EPA 744-R-00-010, United States Environmental Protection Agency, Washington D.C.

WYLIE, A.G. (1988): Relationship between the growth habit of asbestos and the dimensions of asbestos fibers. *Mining Eng.* **40**, 1036-1040.

_____ (1993): Modeling asbestos populations: a fractal approach. *Can. Mineral.* **30**, 437-446.

_____ & SCHWEITZER, P. (1982): Effects of sample preparation and measuring techniques on the shape and shape characterization of mineral particles: the case of wollastonite. *Environ. Res*. **27**, 52-73.

_____ & VERKOUTEREN, J.R. (2000): Amphibole asbestos from Libby, Montana: aspects of nomenclature. *Am. Mineral.* **85**, 1540-1542.

Received August 17, 2002, revised manuscript accepted September 17, 2003.